2010 Highlights

NASA ENERGY AND WATER CYCLE STUDY

NEWS

NEWS Challenge:

Document and enable improved, observationally-based, predictions of water and energy cycle consequences of Earth system variability and change.

Program Manager: J. Entin (NASA-HQ)
Project Scientist: P. Houser (GMU)
Project Office: R. Schiffer (UMBC/GEST) &
Focus Area Liaison: D. Belvedere (UMBC/GEST)

NEWS Working Group Co-Chairs
Drought & Flood Extremes: X. Dong & Y. Deng
Evaporation & Latent Heating: J. Famiglietti & C.A. Clayson
Energy & Water Cycle Climatology: M. Rodell & T. L'Ecuyer
Modeling & Water Cycle Prediction: M. Bosilovich & Y. Hu

Want more NEWS? http://www.nasa-news.org

The Water and Energy Cycle

Is the water cycle accelerating?

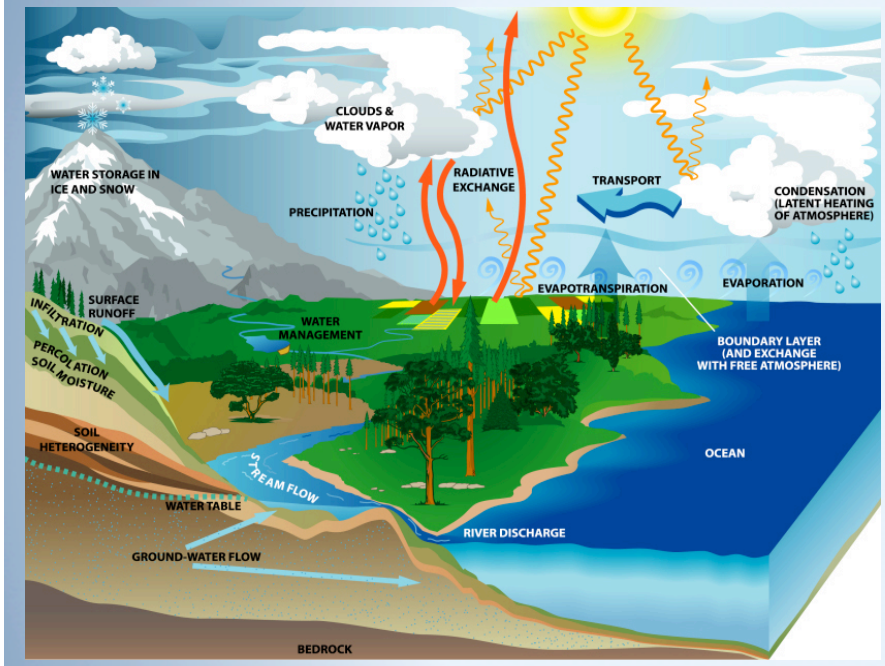

Why NEWS?

Need the collective of NASA & community information and expertise to ask (and define) the larger questions

(aka) Need the whole to be more than the sum of the parts

Why study the water & Energy cycle?

1. *Water exists in all three phases in the climate system and the phase transitions are a significant factor in the regulation of the global and regional energy balances*
2. *Water vapor in the atmosphere is the principal greenhouse gas and clouds at various levels and composition in the atmosphere represent both positive and negative feedback in climate system response*
3. *Water is the ultimate solvent and global biogeochemical and element cycles are mediated by the dynamics of the water cycle*
4. *Water is the element of the Earth system that most directly impacts and constraint human society and its well-being.*

NEWS Publication Highlight

B. Lin, L. Chambers, P. Stackhouse Jr., B. Wielicki, Y. Hu, P. Minnis, N. Loeb, W. Sun, G. Potter, Q. Min, G. Schuster, and T.-F. Fan, Estimations of climate sensitivity based on top-of-atmosphere radiation imbalance, Atmos. Chem. Phys., 10, 1923–1930, 2010. (Published: 19 February 2010)

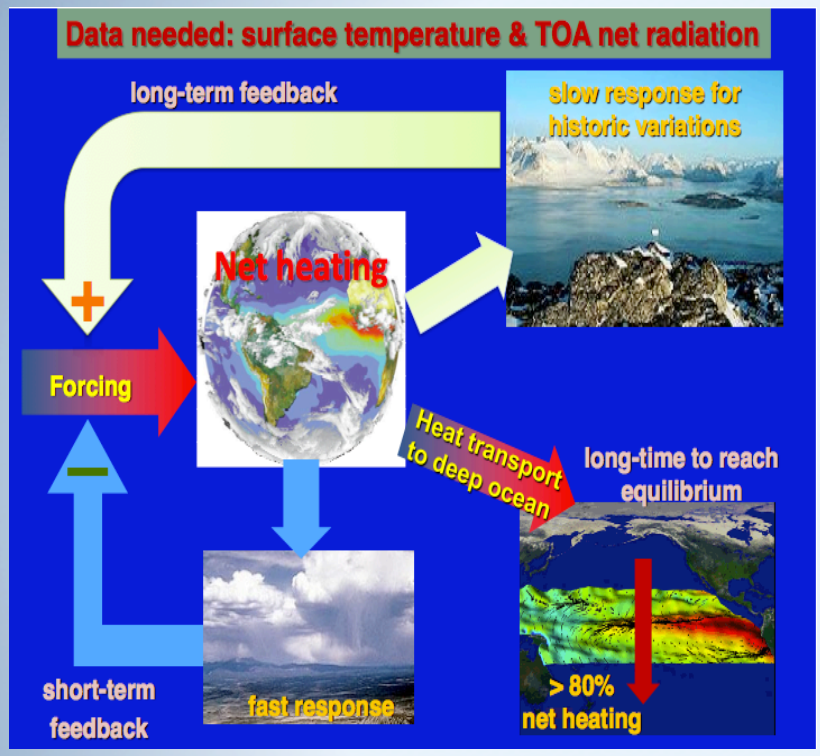

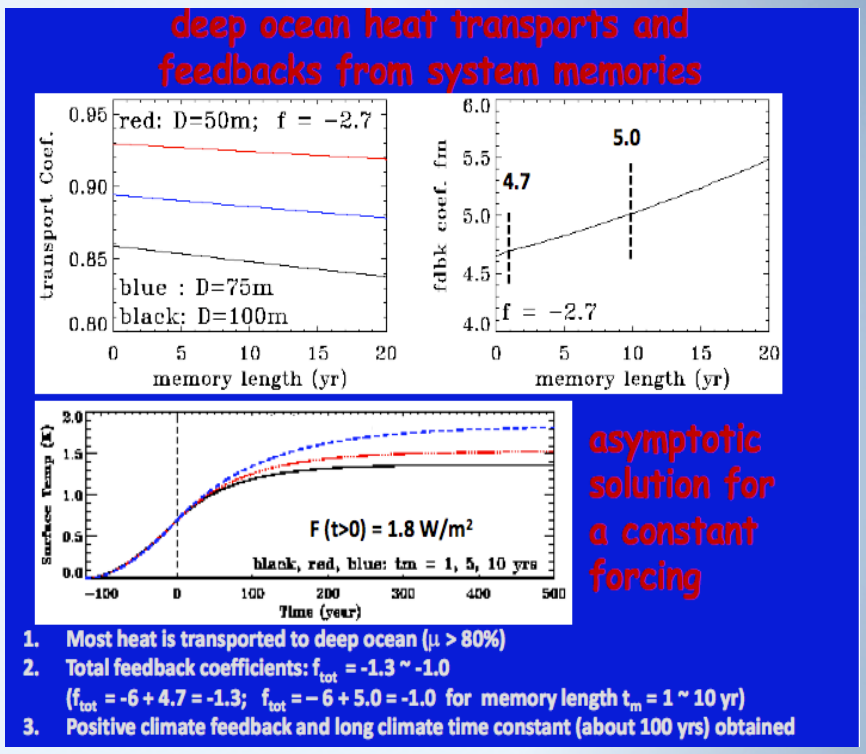

This is a **breakthrough study** that provides observationally-based method to reduce the uncertainties in climate predictions, especially in climate sensitivity and climate feedbacks. This study uses energy balance analysis to estimate the climate sensitivity. **The significance of current analysis is that top-of-atmosphere radiation and surface temperature observations are used as the basis for the estimations of climate feedbacks**. **Additionally, historic climate variations and deep ocean heat transport are considered. This study results in a long time-scale (~ 100 years) of climate system for its changes and variations, which may suggest additional warming beyond what have been seen during last decade for future climate.**

Lin – extra slide

B. Lin, L. Chambers, P. Stackhouse Jr., B. Wielicki, Y. Hu, P. Minnis, N. Loeb, W. Sun, G. Potter, Q. Min, G. Schuster, and T.-F. Fan, Estimations of climate sensitivity based on top-of-atmosphere radiation imbalance, Atmos. Chem. Phys., 10, 1923–1930, 2010. (Published: 19 February 2010)

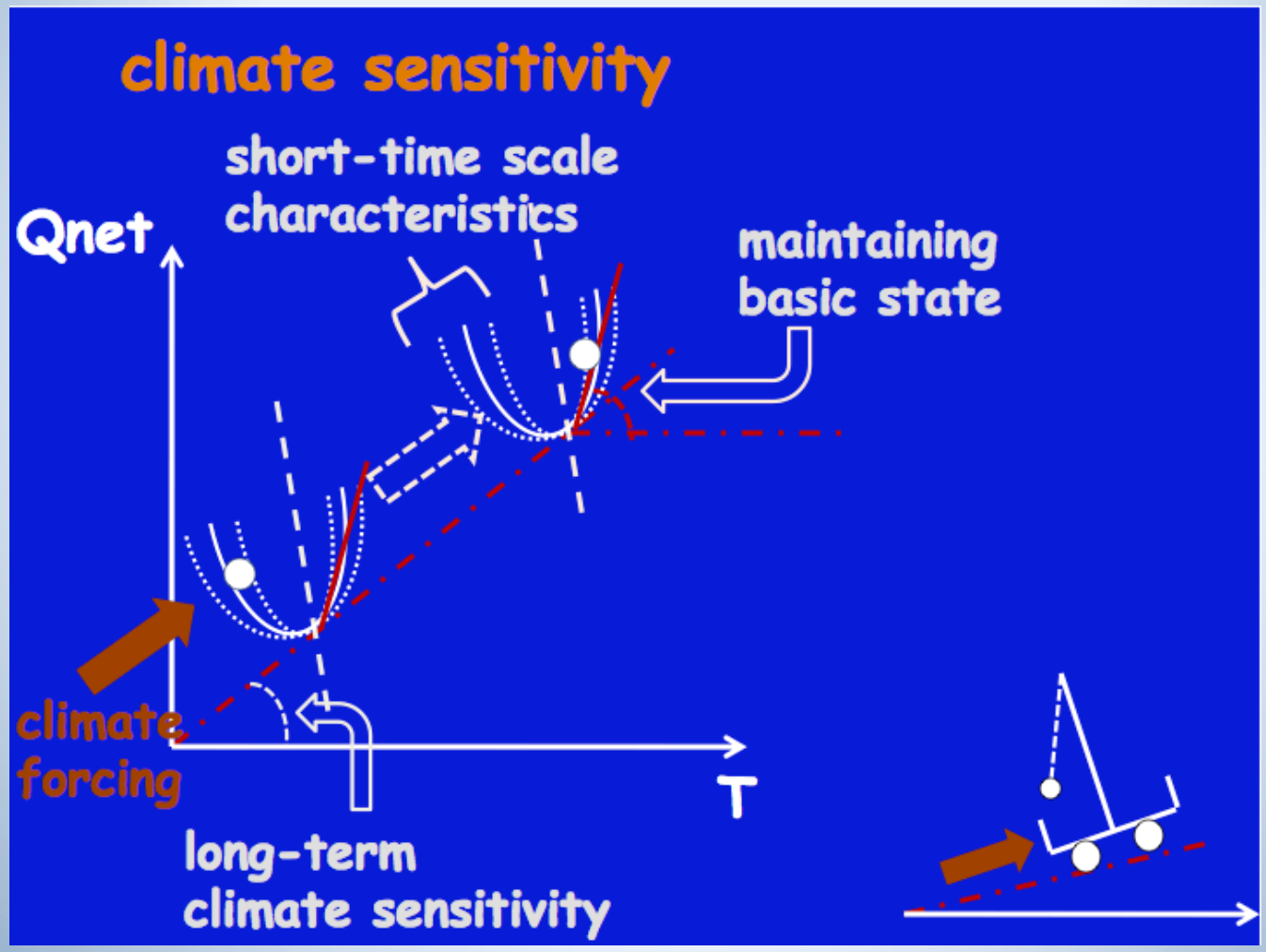

NEWS Publication Highlight

Ozdogan, M., M. Rodell, H.K. Beaudoing, and D. Toll, Simulating the effects of irrigation over the U.S. in a land surface model based on satellite derived agricultural data, J. Hydrometeor., 11 (1), 171-184, doi: 10.1175/2009JHM1116.1, 2010.

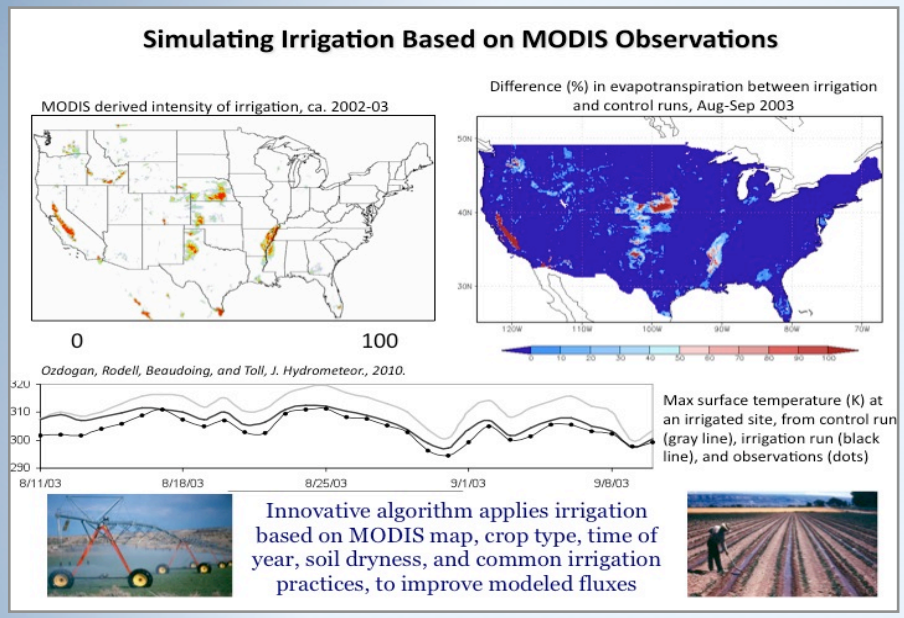

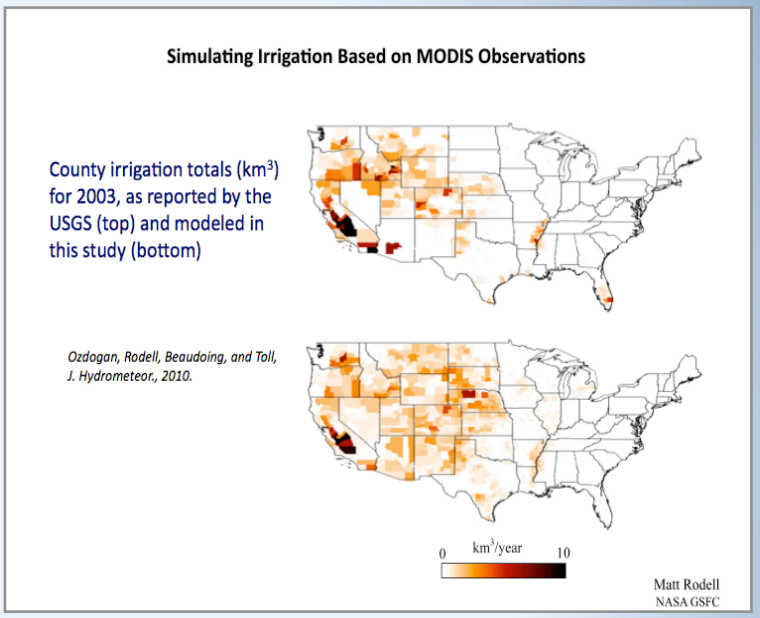

This paper presents a novel scheme for representing irrigation in land surface models, which are the land component of weather and climate forecast models. We used a high resolution map of irrigation intensity derived from the Moderate Resolution Imaging Spectroradiometers (MODIS) aboard NASA's Terra and Aqua satellites. This we integrated into NOAA's land surface model at the scale of the continental United States. **Based on county irrigation totals reported by the USGS, we confirmed that the scheme reasonably estimated the amount of water irrigated**. **We then showed that application of the new irrigation scheme significantly influenced the modeled surface water and energy balances.** Irrigation caused a 12% increase in evapotranspiration and an equivalent reduction in the sensible heat flux averaged over all irrigated areas in the continental US during the 2003 growing season. Local effects were often much more extreme. **We expect that better representation of irrigation will lead to improved weather and climate forecasting skill when the new irrigation scheme is incorporated into numerical weather prediction models such as NOAA's Global Forecast System. Further, the scheme will help to quantify the effects of irrigation on the global water and energy cycles.**

NASA ENERGY AND WATER CYCLE STUDY
NEWS

Vertical Heating Structures Associated with the MJO as Characterized by TRMM Estimates, ECMWF Reanalyses and Forecasts

Integration work in progress

X. Jiang, D. Waliser, W. Olson, W.-K. Tao, T. L'Ecuyer, J.-L. Li, B. Tian, Y. Yung, A. Tompkins, S. Lang, M. Grecu

Motivation: **The Madden-Julian Oscillation (MJO) exerts significant influences on global climate and weather systems. Current GCMs, however, are incapable of robustly representing this form of variability.** To help address this challenge, in particular, considering the potential pivotal role of latent heating in the propagation and maintenance of the MJO, **vertical heating structures associated with the MJO were analyzed by utilizing recently updated heating estimates based on the Tropical Rainfall Measuring Mission (TRMM) from two different latent heating estimates (Olson, Tao) and one radiative heating estimate (L'Ecuyer)**. Heating structures from two different versions of estimates based on the European Centre for Medium-Range Weather Forecasts (ECMWF) reanalyses (ERA-40)/forecasts (EC-IFS) are also examined.

Results:

(1) **The results suggest that diabatic heating (cooling) associated with the MJO convection in the ECMWF outputs exhibits much stronger amplitude and deeper structures than that in the TRMM estimates over the equatorial eastern Indian Ocean and western Pacific. Further analysis illustrates that this difference might be due to stronger convective and weaker stratiform components in the ECMWF estimates relative to the TRMM estimates.**

(2) Despite marked differences in their seasonal mean fields, **the vertical anomalous heating structures reasonably resemble each other based on the four products, including the amplitudes and vertical structures (see right)**.

3) **Analysis illustrates that the stratiform fraction of total rain rate varies with the evolution of the MJO. Stratiform rain ratio over the Indian Ocean is found to be 5% above (below) average for the disturbed (suppressed) phase of the MJO.**

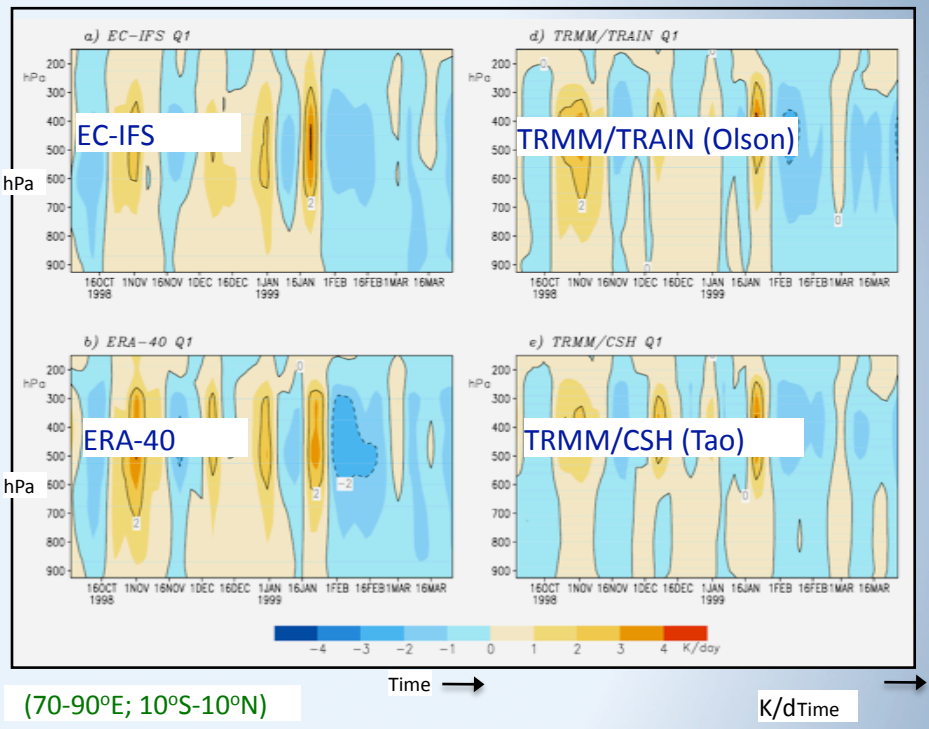

Time-pressure structures of anomalous heating (units: K day^{-1}) during the 1998/99 winter based on EC-IFS forecast, ERA-40 reanalysis, TRMM/TRAIN, TRMM/CSH estimates. All fields are averaged over the equatorial eastern Indian Ocean (75-95°E; 10°S-10°N). Anomalies are calculated with relative to their corresponding seasonal mean values during Oct. 1998 – Mar. 1999

Analysis links Atmospheric Rivers and Snow Accumulation in the Sierra Nevada

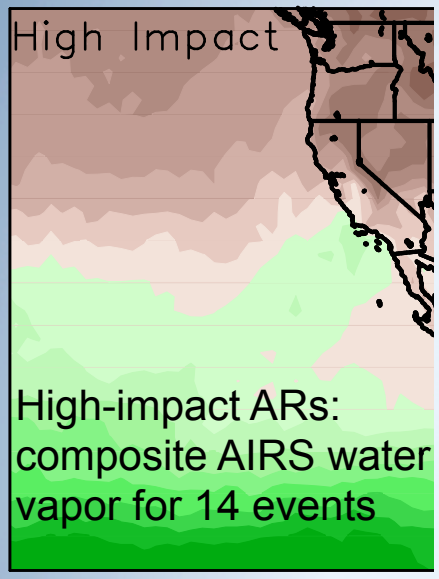

MODIS-model recon SWE

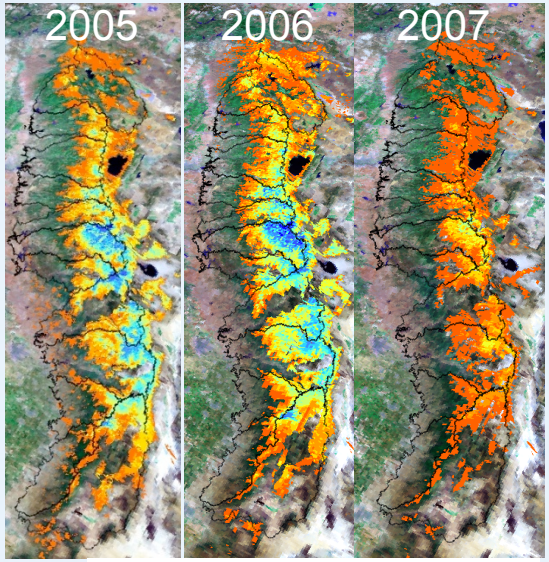

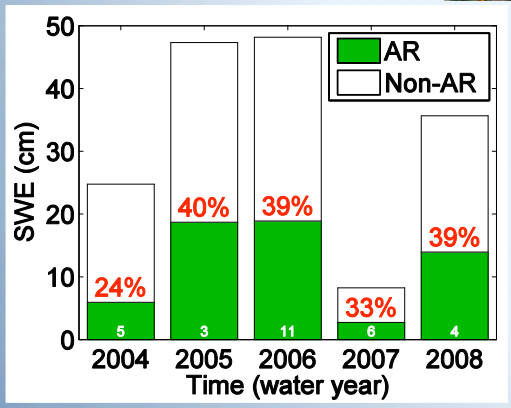

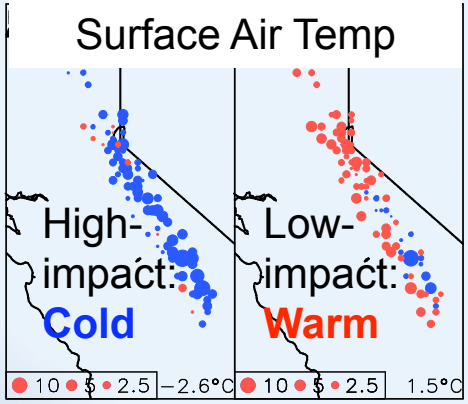

Problem: Atmospheric rivers (Ars) are narrow corridors of concentrated moisture in the atmosphere, and are a key process linking weather and climate. **ARs, typically a few events in a single winter, may result in up to ~40% of the total seasonal snow accumulation in the Sierra Nevada. It is not well understood what makes some events more influential than others.**

Result: Analysis of in-situ data reveals close connection between mountain surface air temperature (SAT) and amount of snow accumulation during ARs. Such connection is seen well tracked by NASA satellite AIRS (Atmospheric Infrared Sounder) L3 temperature retrievals.

Significance: The result suggests potential utility of AIRS temperature products and the snow water equivalent (SWE) reconstruction product in understanding/predicting the impacts of landfalling ARs on water resources.

Guan, Molotch, Waliser, Fetzer, and Neiman, to be submitted to *GRL*

Modeled downward radiative flux at the surface from the atmosphere increases due to CALIPSO CludSat derived cloud base

One of the improvements CALIPSO and CloudSat data provide is accurate vertical cloud profiles. The downward surface irradiance, especially longwave, is sensitive to the cloud base height. Active sensor (Calipso and CloudSat) derived cloud base heights increase the modeled global annual mean downward surface longwave radiative flux by 2 to 3% (~7Wm^2) compared with the radiative flux computed without the active sensors; i.e. **the surface receives 2-3% more radiation from the atmosphere. Because the global mean net surface radiative flux balances the surface latent and sensible heat fluxes and ocean heating, *it will reduce the uncertainty in the global surface energy budget.***

Figures 1 and 2 demonstrate the improvements. The change of the downward surface longwave irradiance is larger in midlatitude and polar regions because of small column water vapor amounts.

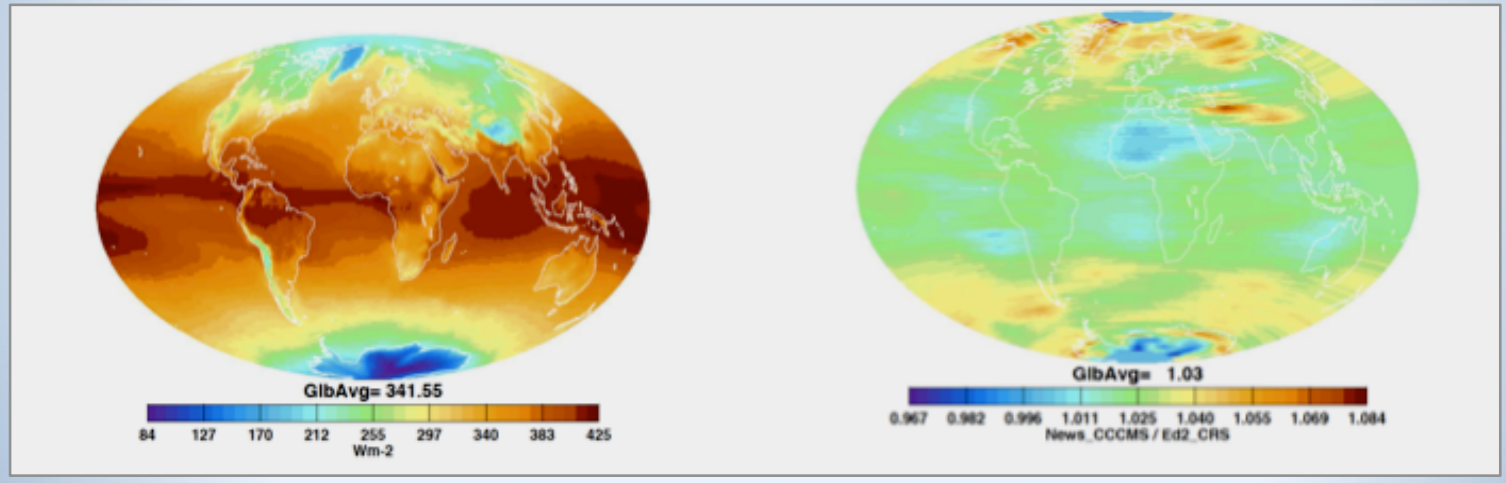

Figure 1: Annual mean (July 2003 through June 2004) downward surface longwave irradiance computed with MODIS derived cloud properties. GEOS-4 temperature and humidity profiles were used.

Figure 2: The ratio of the surface downward longwave irradiance computed with CALIPSO and CloudSat derived cloud vertical profiles to that computed with MODIS derived cloud only. **The global mean surface longwave irradiance increase by ~30% when CALIPSO and CloudSat derived clouds are used**

Wielicki, Kato

Are climate-related changes to the character of global-mean precipitation predictable?

The study suggests that the latent heat release due to changes in global rainfall is balanced primarily by the changes in radiative cooling by water vapor. Although water vapor may increase 6% per degree warming, the radiative cooling by increased water vapor only increased about 1-2% since the water vapor absorption line centers are saturated and the extra cooling is due to changes in the weak absorption part of the absorption spectrum. The theory agrees well with GCM results.

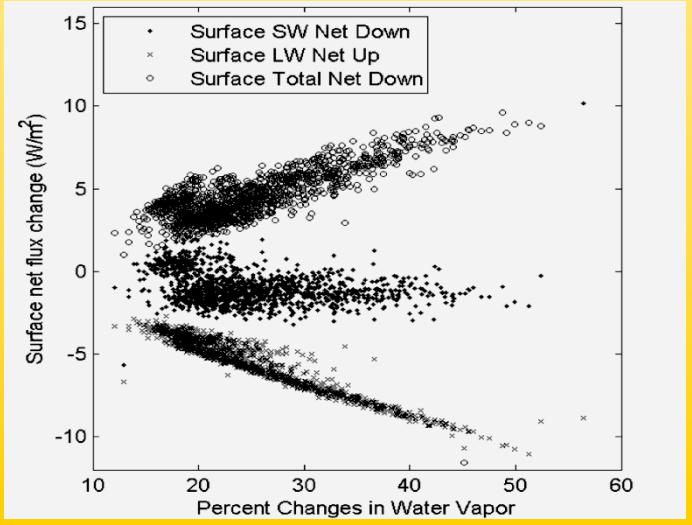

Fig.1: changes in net SW, LW and total (SW+LW) net surface fluxes as a function of the percent change in water vapor.

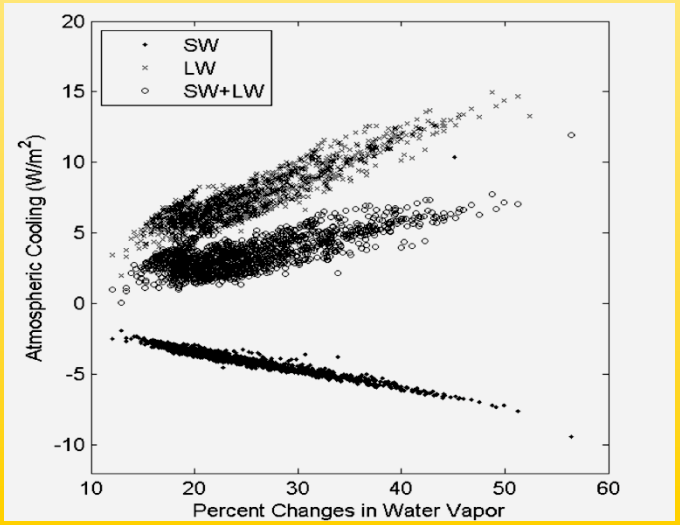

Fig.2: changes in net SW, LW and total (SW+LW) net surface fluxes as a function of the percent change in water vapor **but for a change in atmospheric radiative heating. (**Total LW radiative cooling is about 100 W/M^2**)**

G. Stephens and Hu ,Y. (2010), Are climate-related changes to the character of global-mean precipitation predictable? *Environ Res Lett , submitted.*

Are climate-related changes to the character of global-mean precipitation predictable?

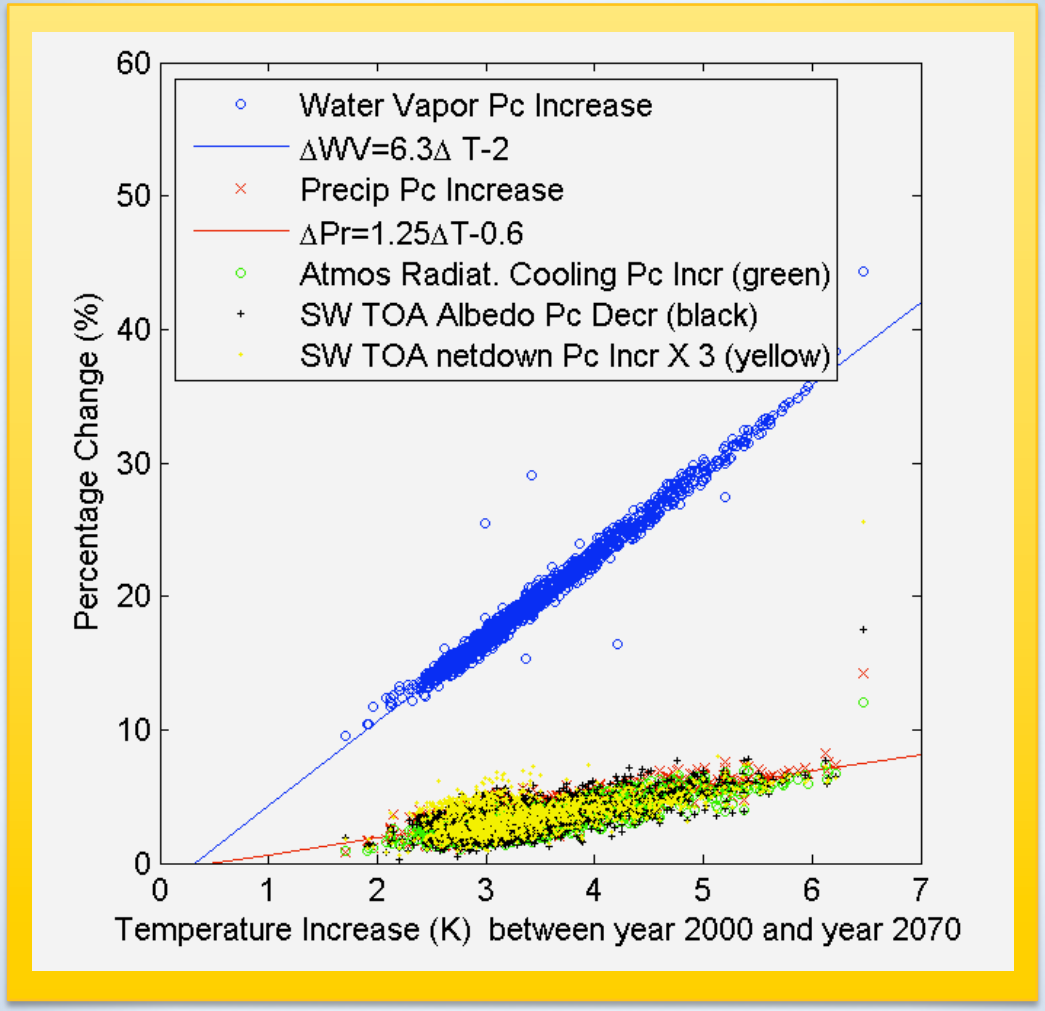

Figure 3. Water vapor at boundary layer (blue) increase about 6.3% per degree warming. Precipitation (red), atmospheric radiative cooling (green), TOA shortwave wave albedo (black) increase roughly about 1.25% per degree warming.

Diurnal Cycle of Summer Precipitation over US

	Satellite (1998-2005)	fvGCM (1998-1999)	MMF (1998-1999)
Precipitation Frequency	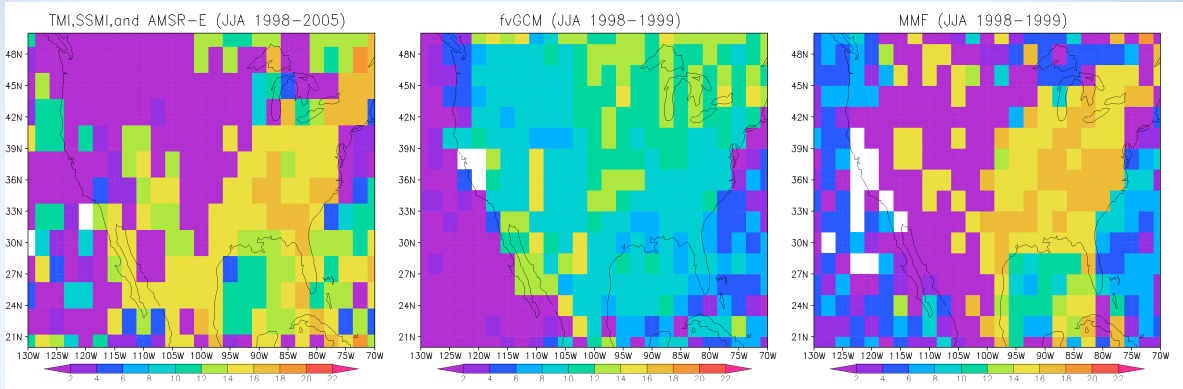		
Precipitation Intensity	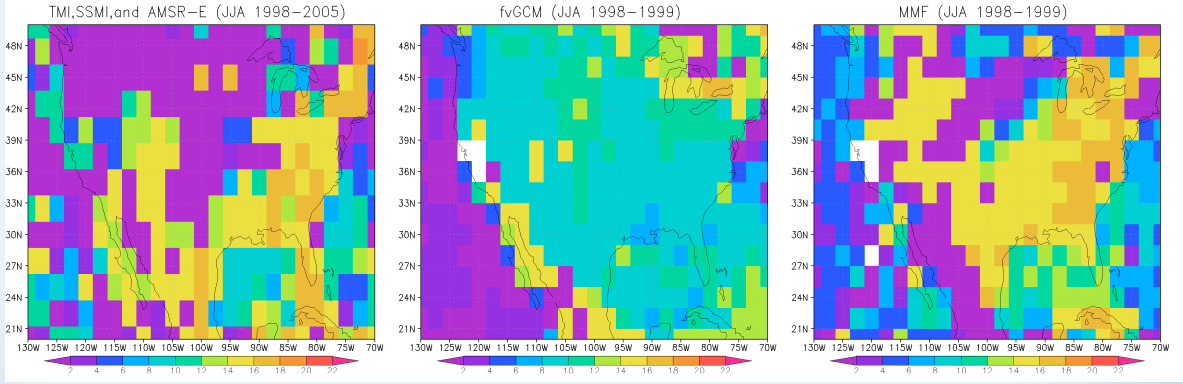		

Figure. The diurnal cycle is a fundamental mode of atmospheric variability and has a major impact on weather and climate prediction. However most convectional global models have a problem simulating the timing of diurnal cycle of precipitation. **The figure shows that multi-scale modeling framework (MMF) results substantially improve the timing of maximum precipitation frequency and intensity over the United States when compared with the merged microwave satellite observations.** (The color bar indicates the local time of the maximum rain frequency and intensity.)

Multiscale Simulation during Twin Tropical Cyclogenesis (TCs), a low pressure area, associated with a Large-scale MJO

•Accurate predictions of multiple tropical cyclones in location and timing would require a numerical model to simulate global water cycle realistically, as moist processes associated with precipitation and surface flux exchange provides the energy source that fuels the formation and intensification of TCs.

• *Figures below show* ***predictions regarding the formation of twin tropical cyclones in the Indian Ocean,*** **demonstrating the modeling ability to do tropical cyclones** - key atmospheric processes to transport water and energy from tropical to mid-latitude, and modeled diurnal variation that almost all climate models cannot do.

0630 UTC 1 May 2002

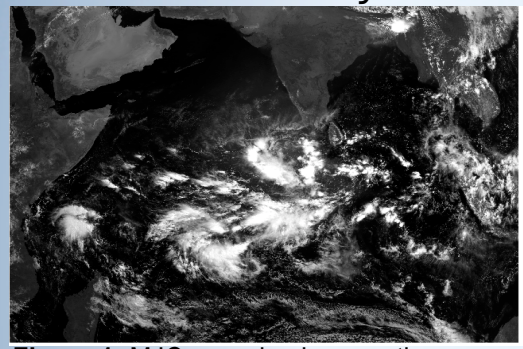

Figure 1: MJO-organized convection over the Indian Ocean at 0630 UTC 1 May 2002.

0000 UTC 6 May 2002

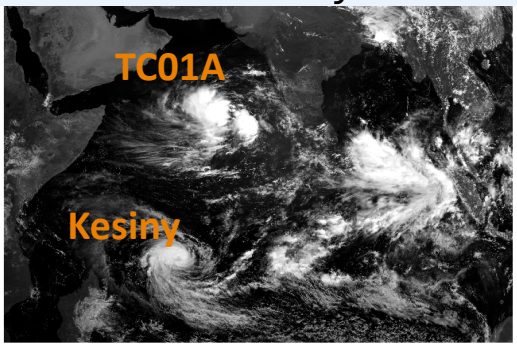

0000 UTC 9 May 2002

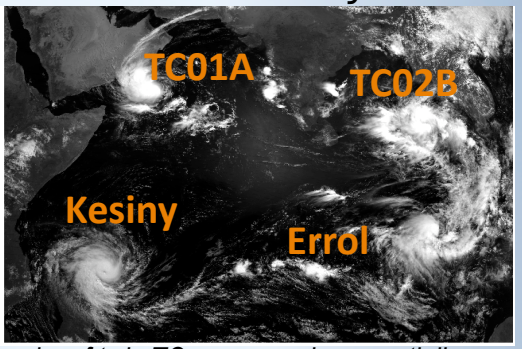

Figure 2 & 3: *When the MJO moved eastward, two pairs of twin TCs appeared sequentially on 6 May (2) and 9 May (3), including TC 01A, Kesiny, TC 02B and Errol. Two TCs (01A and 02B) with anti-clockwise circulation appeared in the Northern Hemisphere, while two TCs (Kesiny and Errol) with clockwise circulation in the Southern Hemisphere*

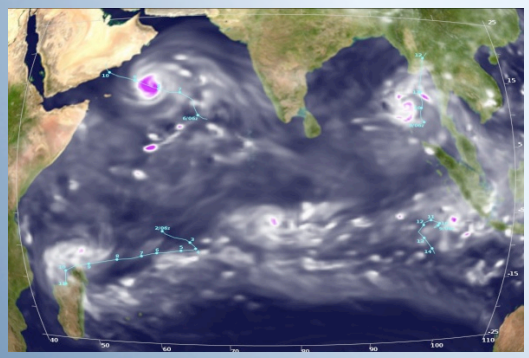

Figure 1 (left): Four-day forecasts of total precipitable water, showing realistic simulations of TC's formation and movement (see Shen et al., 2010 for details).

Shen, B.-W., W.-K. Tao, R. Atlas, Y.-L. Lin, C.-D. Peters-Lidard, J.-D. Chern, K.-S. Kuo, 2009: Forecasting Tropical Cyclogenesis with a Global Mesoscale Model: Preliminary Results for Twin Tropical Cyclones in May 2002. (to be submitted)

Precipitation Simulations associated with Twin Tropical Cyclogenesis

(a) NASA TRMM

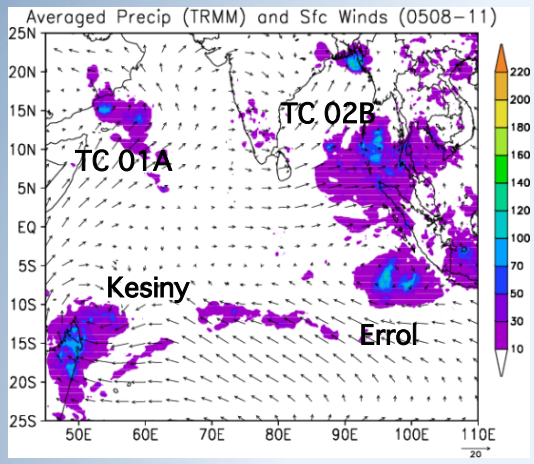

(b) CNTL

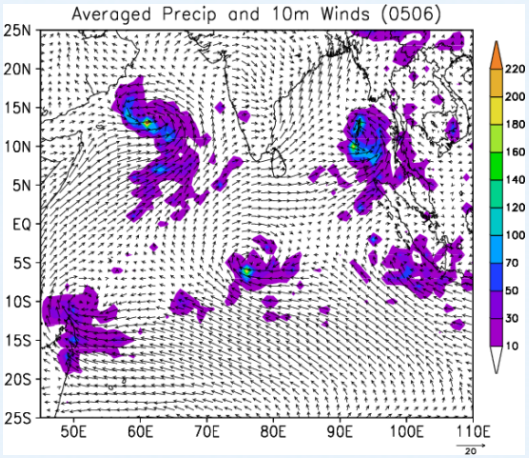

(c) EXP-A

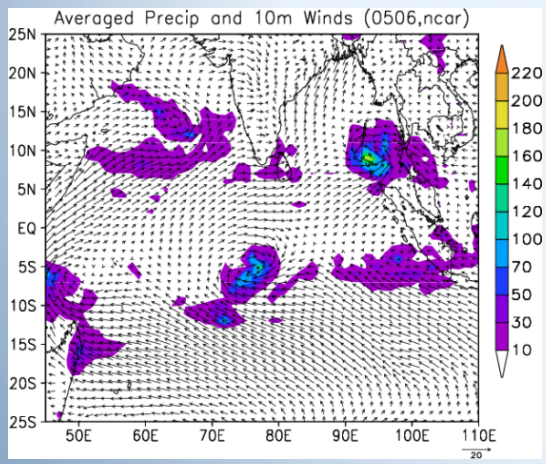

(d) EXP-B

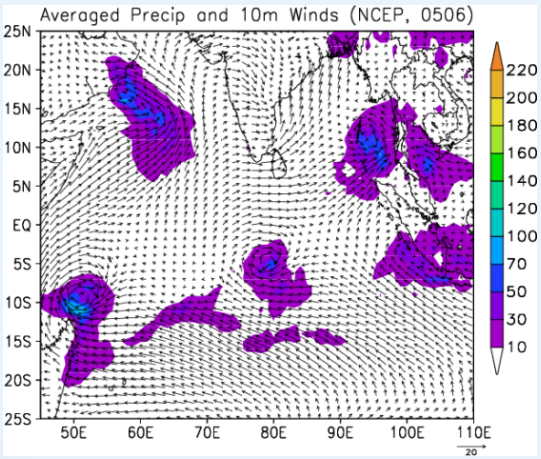

Precipitation (mm/day) averaged over May 8-11, 2002 from (a) NASA TRMM, (b) the control run (labeled as CNTL) and two parallel runs for (c) the exp-A run and (d) the exp-B run. All of three runs are initialized at 0000 UTC May 6, 2002 with different moist physical processes. Case CNTL has no cumulus parameterizations. Case EXP-A has Zhang and McFarlane (1995) and Hack (1994) schemes for deep and shallow-and-midlevel convection, respectively. Case EXP-B uses NCEP SAS (simplified Arakawa and Schubert) scheme (Pan and Wu 1995). The false-alarm event appears in all of three runs, suggesting missing physical processes in the model or imperfect Ics.

Shen, B.-W., W.-K. Tao, R. Atlas, Y.-L. Lin, C.-D. Peters-Lidard, J.-D. Chern, K.-S. Kuo, 2009: Forecasting Tropical Cyclogenesis with a Global Mesoscale Model: Preliminary Results for Twin Tropical Cyclones in May 2002. (to be submitted)

Determining Vertical Structure from Geostationary Satellite Data Using Cluster Analysis and Statistical Classification

Knowing the vertical structure of clouds is an important element in understanding their radiative impact and is important for evaluating climate models. Cloud radars provide detailed view of cloud vertical structure but have limited spatial sampling while geostationary satellites have large spatial view but limited vertical information; combining them can produce cloud vertical information on large spatial scales. We used a clustering methodology to derive characteristic vertical structure of clouds and their heating profiles from ground radar observations (left). Classification matrix (right) shows geostationary satellite data plus simple information from reanalysis datasets can be used to predict which cluster an observation falls into ~77% of the time - indicating ability to predict vertical structure from geostationary satellite observations.

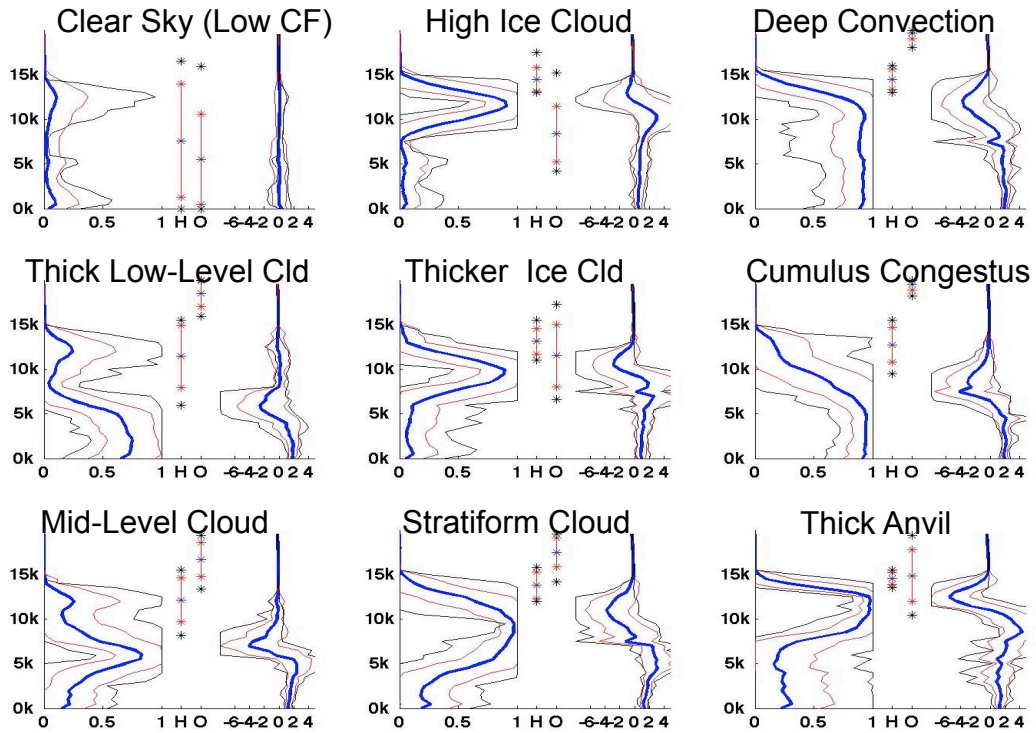

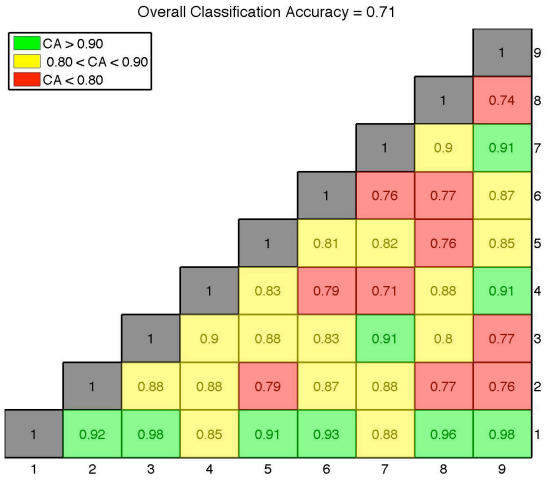

McFarlane, Beagley, Flaherty

NASA ENERGY AND WATER CYCLE STUDY

High-Resolution Satellite Surface Latent Heat Fluxes in North Atlantic Hurricanes

Latent Heat Flux (W m^{-2})

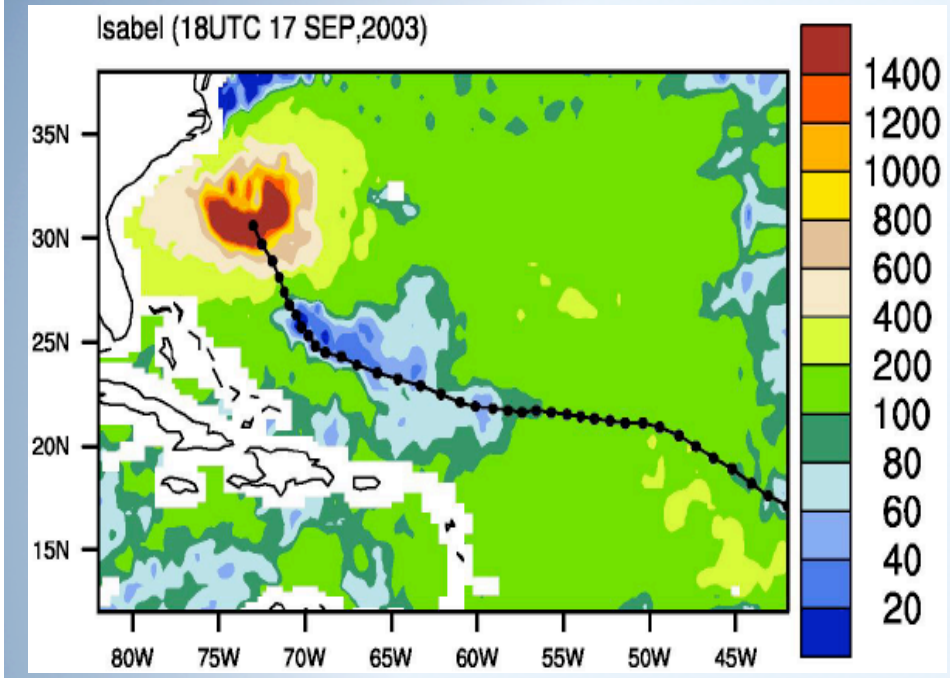

Sea Surface Temperature (° C)

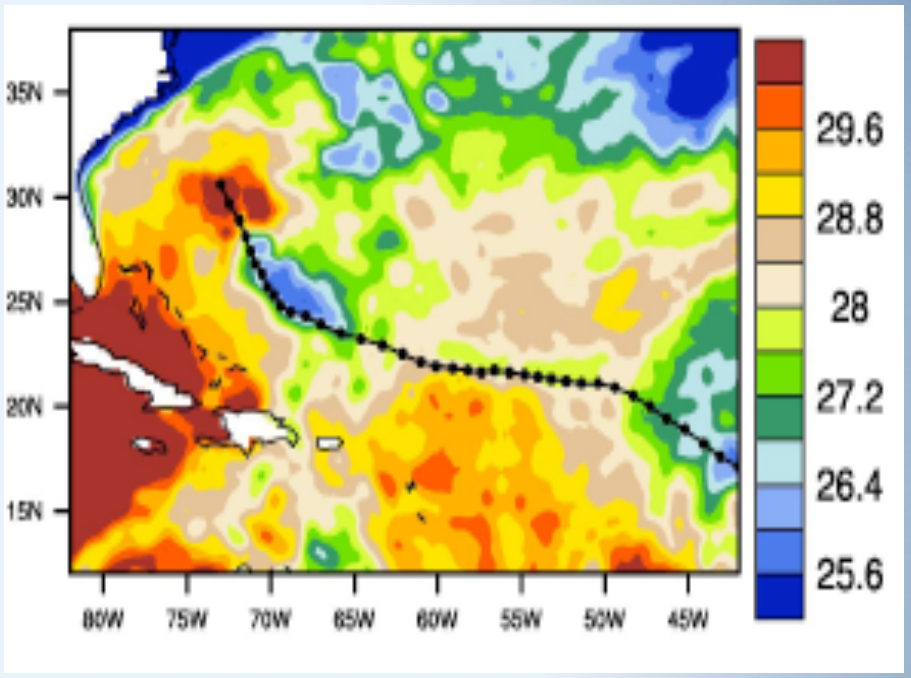

Satellite data sources: AVHRR, AMSR-E, SSM/I, TMI, QuikSCAT, AMSU-A

As part of the NEWS program, a new high resolution ocean surface latent heat flux data set has been developed that is capable of reproducing the extreme heat fluxes occurring in hurricanes. This snapshot of Hurricane Isabel shows the very high latent heat fluxes in the hurricane, plus the cold wake behind hurricane, and the vastly diminished latent heat fluxes. **This high-resolution dataset is being used to improve understanding of hurricane energetics and the impact of hurricanes on the upper ocean.**

Curry, J. Liu, Clayson, Bourassa

4/2/10

NASA ENERGY AND WATER CYCLE STUDY NEWS

Global Energy Balance Archive (GEBA) Downward Shortwave Radiation (DSW)

trend analysis over the Arctic: from Dimming to Brightening

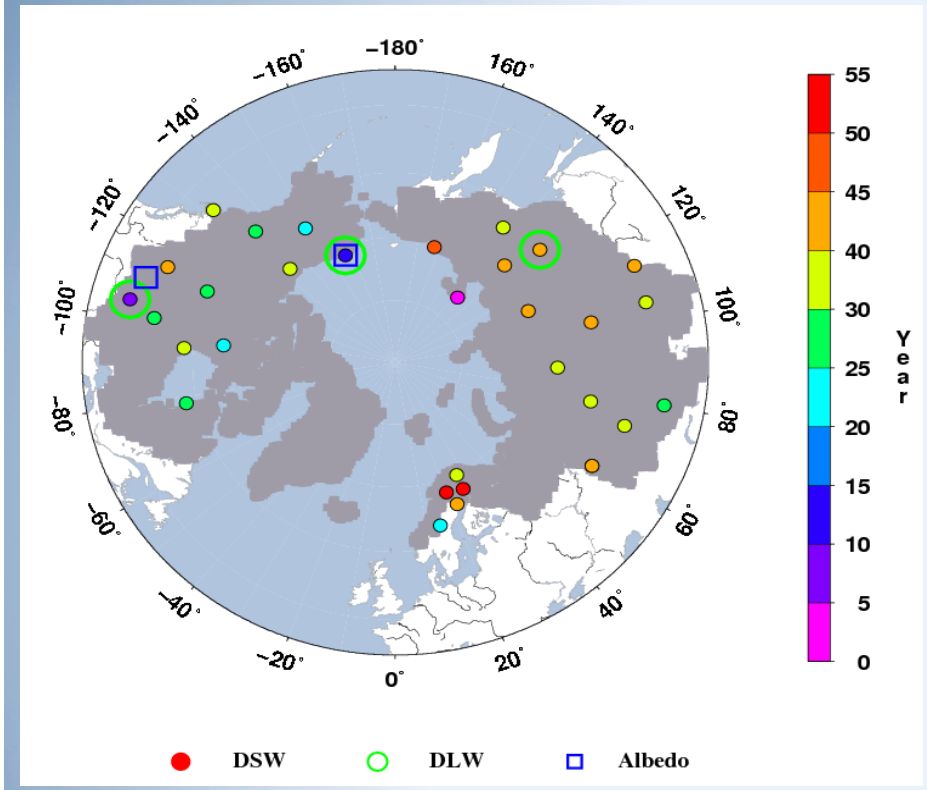

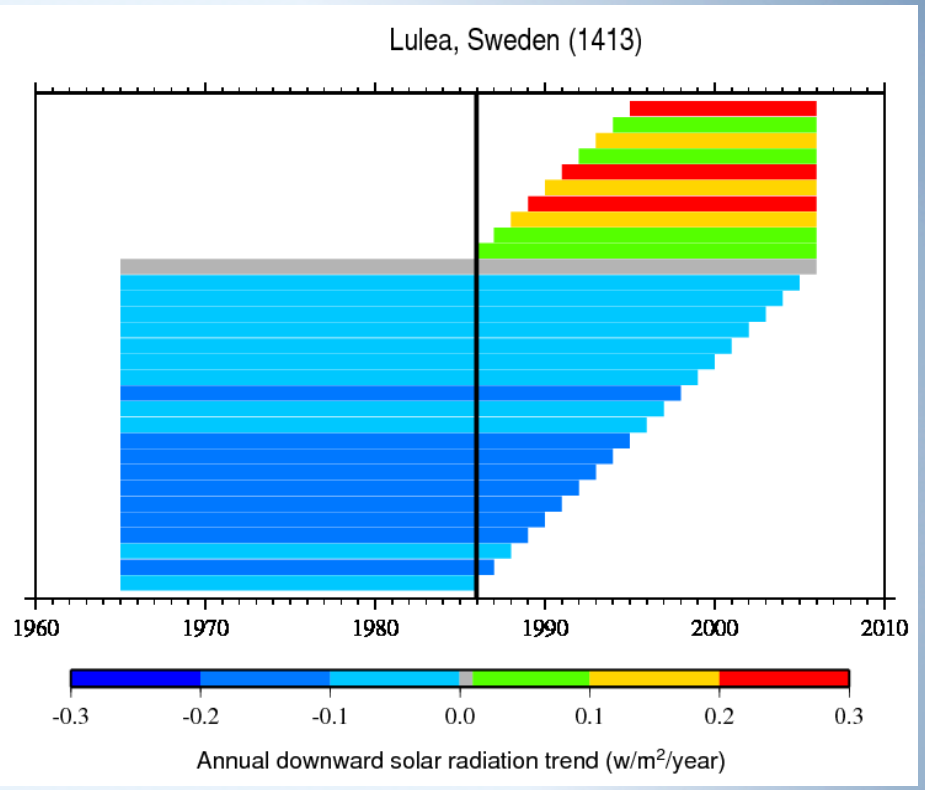

32 DSW stations from **Global Energy Balance Archive (GEBA)**

No trend (1965~2006) = Decreasing trends + Increasing trends

Apparently, there is a turning point which is between 1985 and 1990 at these sites. Before that, a dimming period exists with decreasing trends, whereas brightening occurred thereafter. The role and importance of changes in surface solar radiation have been widely discussed, particularly with respect to documented changes in arctic snow cover. **This work offers a definitive evaluation of the nature of changes over the last 40+ years, and shows that while over the early part of the record, there was dimming, more recently there have been compensating increases, such that over the entire period, there is no net trend.**

Lettenmaier

NASA ENERGY AND WATER CYCLE STUDY NEWS

4/2/10

MK trend test results for annual DSW observations

GEBA ID	Station Name	Start Year	End Year	Annual	
				P	Trend
396	Edmonton	1950	1987	<0.05	-0.16
442	Whitehorse	1971	1987	<0.01	-0.47
1413	Lulea	1965	2006	---	0.00
2104	Oestersund	1983	2005	<0.01	0.38
2492	Ekaterinburg	1964	1994	<0.05	-0.21
930	Turukhansk	1964	1995	---	-0.04
931	Olimyakon	1964	1992	<0.01	-0.36
932	Yakutsk	1964	1991	---	-0.07
933	Aleksandrovskoe	1964	1993	<0.05	0.30
936	Sverdlovsk	1964	1990	---	-0.01
937	Omsk	1964	1995	---	0.04
940	Irkutsk	1964	1993	---	-0.23

- Trend test: using Mann-Kendall/Sen Slope at a 5% significance level;
- Calculate trends for annual downward shortwave radiation (DSW) of 12 GEBA sites spanning the periods from the 1950s and 1960s to post-2000;

8 (4)

3(2)

1

Lettenmaier

4/2/10

NASA ENERGY AND WATER CYCLE STUDY NEWS

Comparison of intense precipitation days (upper line of plots) and multi-day intense precipitation events (lower line of plots) over the central United States between the 1978-2007 and 1948-1977 periods sorted by day/event intensities

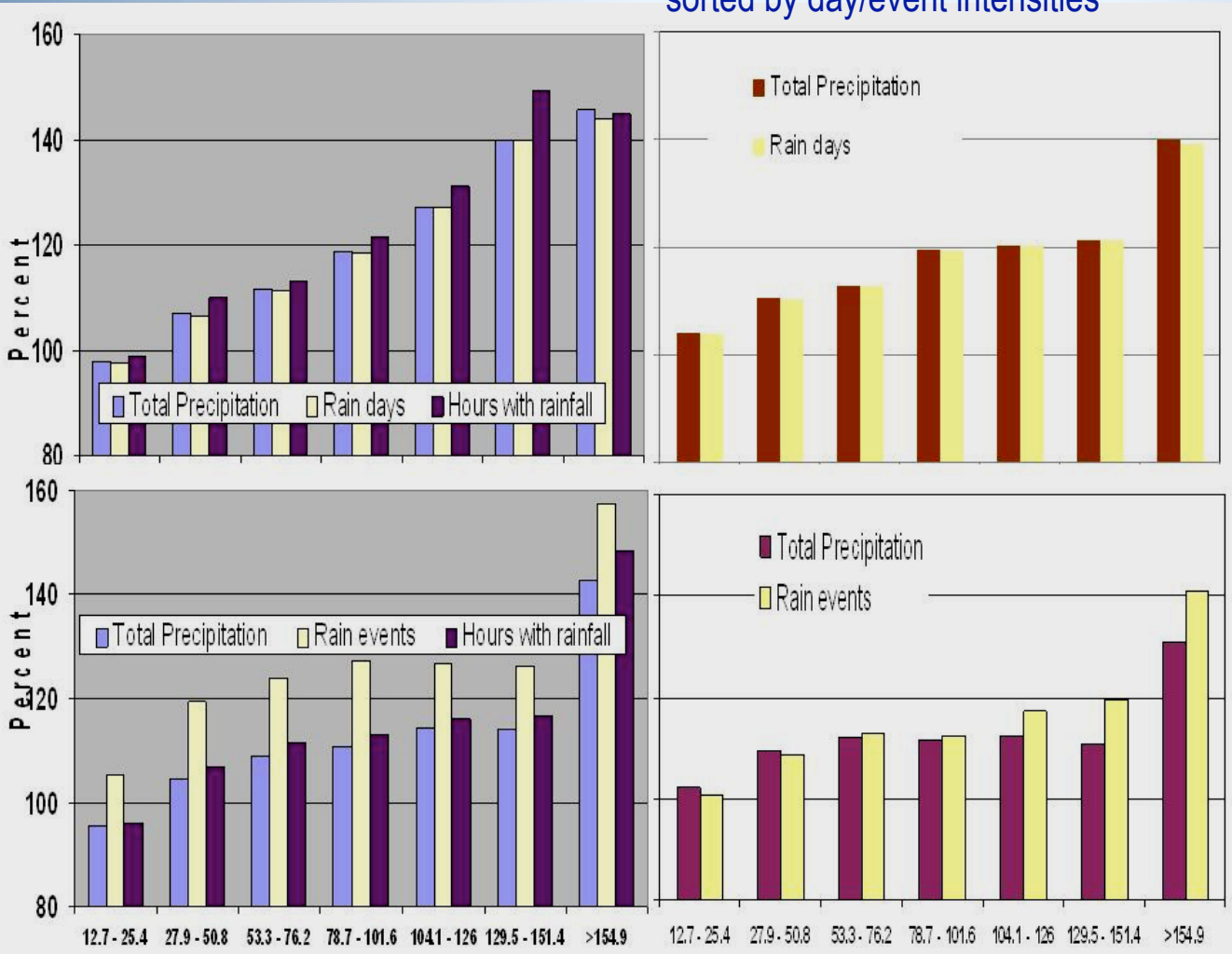

Intense precipitation (above 0.5") encompasses approximately two thirds of annual precipitation totals and about 20% of all rain days over the contiguous United States. In recent decades, high-intensity events (above 1") became more frequent over the nation and, particularly, over the central United States.

Information from studies such as this one may help assess the potential for disasters in the future, and would benefit farmers, politicians, water managers, insurance companies, construction companies... and other scientists.

On the x-axes, plots have the daily precipitation ranges, in mm, selected to accommodate the British units, inches (so, the first category, from 12.7 mm to 25.4 mm corresponds to 0.5" to 1", and the last above 6").

Results are based on two national U.S. data sets. Groisman *et al.* (2010)

NEWS Datasets Shed New Light on the Differences between the Northern and Southern Hemisphere Branches of the ITCZ

Principal Investigator: T. S. L'Ecuyer (tristan@atmos.colostate.edu)

Science Question (Figure 1): TRMM observations show a year-round band of rainfall (called the Inter-Tropical Convergence Zone, ITCZ) just north of the equator in the tropical east Pacific (white box). Why does the second band of rainfall in the southern hemisphere only show up in March-May?

Relevance: More than two-thirds of the heat released in the Earth's atmosphere occurs in the tropics and the ITCZ, in particular, plays a central role in the global circulation and water cycle. The many competing explanations for north-south differences in the ITCZ are all based primarily on numerical models and need to be tested using observations.

Data Integration: This study combines several NEWS data products to determine which sources of ocean heating are responsible for the differences in rainfall north and south of the equator.

Significance: This study resolves the debate about the main sources of equatorial asymmetry using exclusively satellite-based datasets. It also provides an observational benchmark for testing future model predictions. Such tests are essential to increase confidence in future climate predictions.

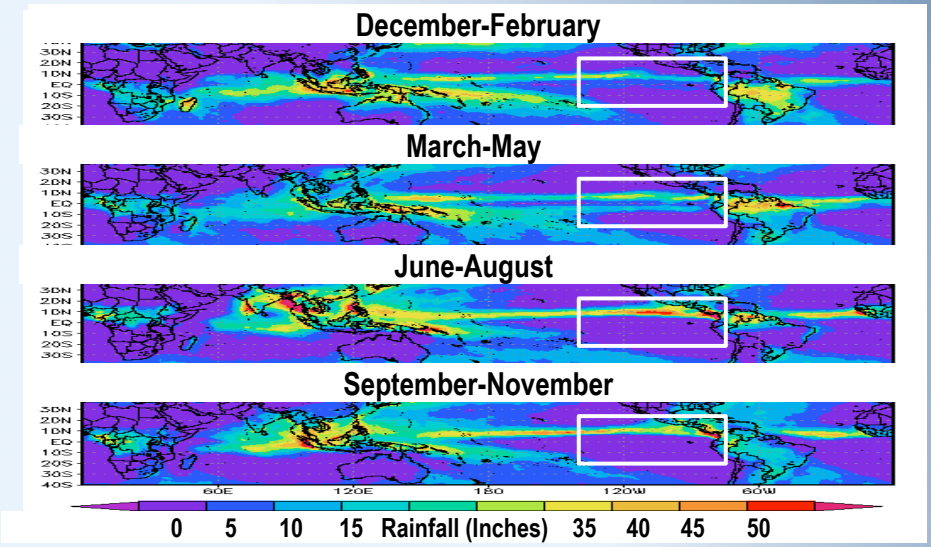

Figure 1: Average rainfall observed by the Tropical Rainfall Measuring Mission (TRMM) in the northern hemisphere winter, spring, summer, and fall seasons..

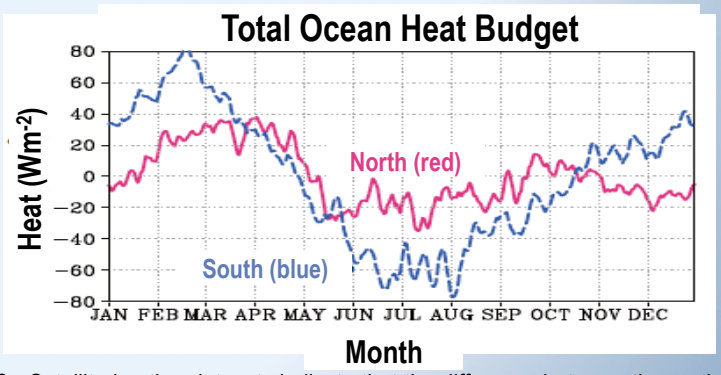

Figure 2: Satellite heating datasets indicate that the difference between the northern and southern hemispheres is caused by much stronger seasonal shifts in the southern ocean's heat budget (the sum of all sources of heating and cooling of the upper ocean). There are three main reasons for this: (a) the Earth is closer to the sun during the southern hemisphere summer months, (b) the ocean is slightly more efficient at absorbing sunlight south of the equator, and (c) increased sunlight during summer months north of the equator is offset by increases in cloudiness that reflect more of this sunlight back to space.

Masunaga, H. and T. S. L'Ecuyer, 2010a: "The Southeast Pacific Warm Band and Double ITCZ", *J. Climate* **23**, 1189-1208.

Masunaga, H. and T. S. L'Ecuyer, 2010b: "Equatorial Asymmetry of the East Pacific ITCZ: Observational Constraints on the Underlying Processes", submitted to *J. Climate*.

5/3/ 2010

Development and diagnostic analysis of a multi-decadal global evaporation product for NEWS

Princeton University
PI: Eric F Wood

NASA ENERGY AND WATER CYCLE STUDY

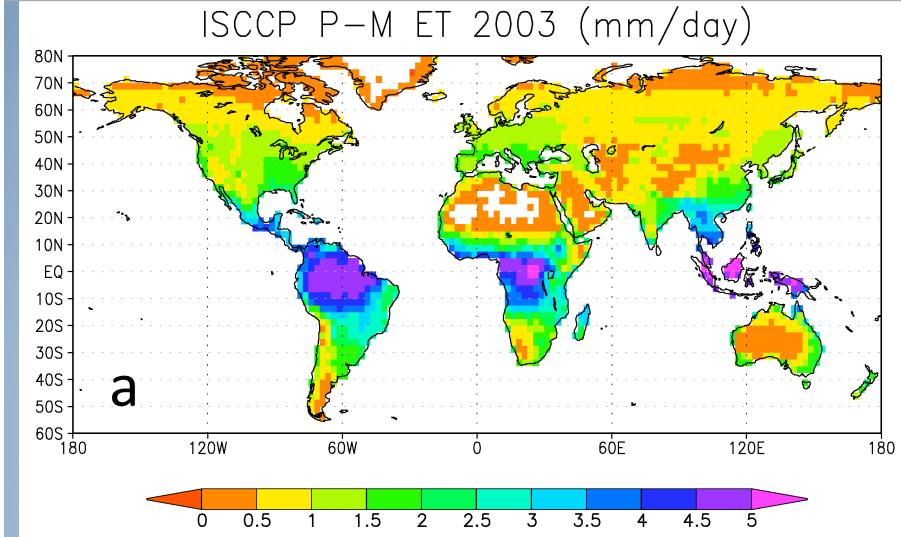

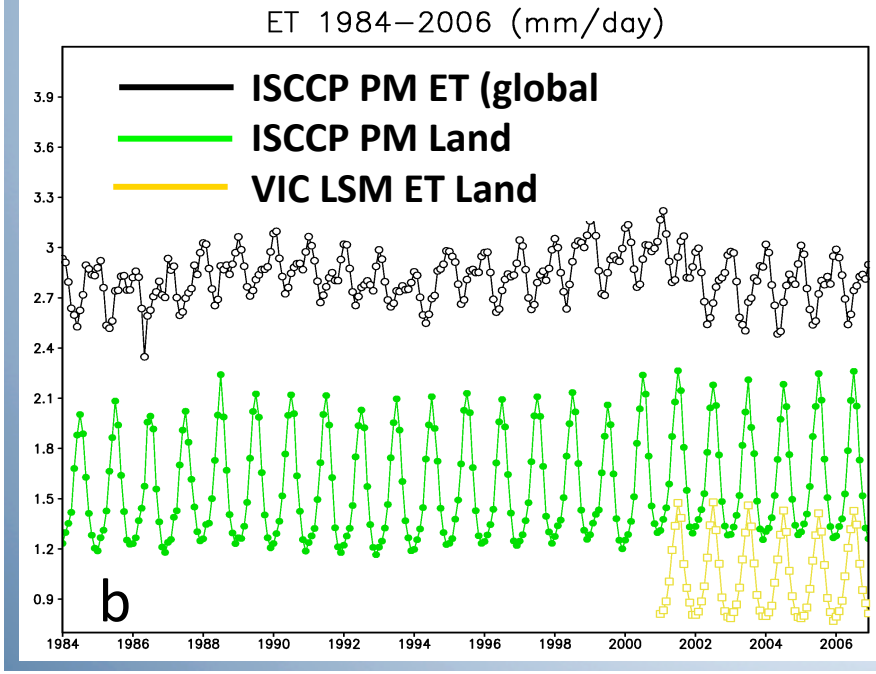

Panel a: Annual terrestrial ET using the ISCCP data and a Penman-Monteith RS model

Panel b: 1984-2007 terrestrial and global ET estimates using PM/ISCCP. Note comparison to VIC LSM and global P ~2.8 mm/day

Panel c: Comparing remote sensing to operational models being assessed by NEWS

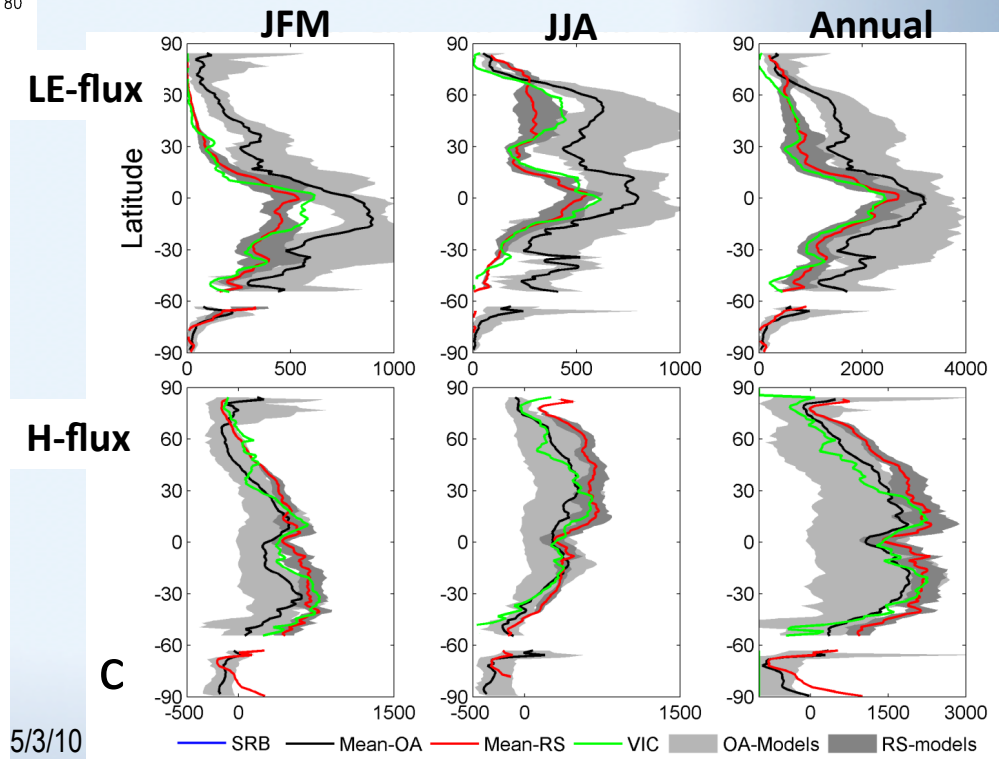

5/3/10

NEWS Publication Highlight

Ye, H., and E. J. Fetzer (2009), **Atmospheric moisture content associated with surface air temperatures over northern Eurasia**, *Int. J. Hydrology*, in press.

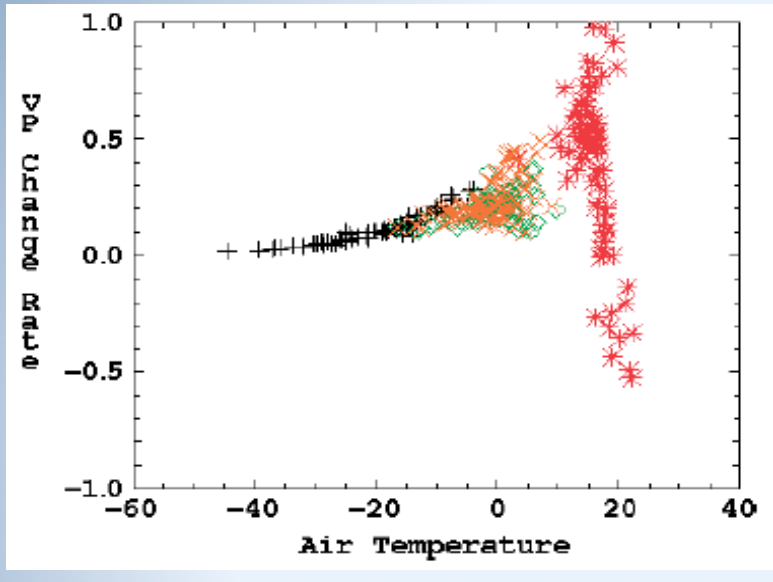

Water vapor partial pressure change per degree of air temperature increase (hPa/°C) versus mean air temperatures for 80 stations for winter (black), spring (green), summer (red), and fall (orange) during 1936–1990.

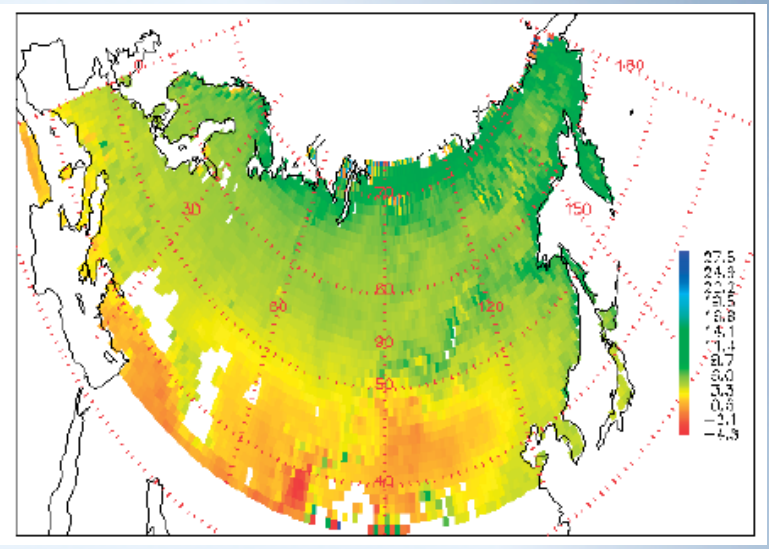

Distribution of the rate of change of AIRS total precipitable water with surface air temperature (%/°C) during 2003-2006.

Lead Author Hengchun Ye received the American Association of Geographers Climate Specialty Group John Russell Mather Paper of the Year Award for this study.

Summary: This paper examines the relationship between surface air temperature and total precipitable water vapor in historical records and AIRS observations over northern Eurasia. In cold conditions total water vapor follows surface air temperature closely. During warmest conditions total water vapor increases slowly with surface air temperature.

Significance: Climate models predict approximately constant relative humidity with temperature. These results show that warmest conditions are associated with lowest relative humidity over Eurasia. **This suggests that climate models may be overestimating the strength of water vapor-driven greenhouse warming at high latitudes during summer**.

Application of a Source-to-Sink Runoff Routing Scheme to Improve Simulated River Discharge

Principal Investigator: Matt Rodell, NASA/GSFC (Matthew.Rodell@nasa.gov)

River discharge is a quantity that integrates all upstream water cycle processes. As such, it is an important indicator of the hydrologic and climatic conditions of a river basin, as well as a useful tool for evaluating hydrologic models.

By applying a source-to-sink (STS) runoff routing scheme to gridded runoff maps generated by a global hydrologic model, we can produce more accurate estimates of discharge from the world's major rivers. These model estimates are particularly valuable in regions where gauge observations are not available.

In a STS scheme, streamflow parameters are estimated a priori, and the algorithm can be applied to modeled runoff as a post process to produce a time series of discharge for each predetermined outflow location. The major advantages of STS over the cell-to-cell routing approach are that STS is computationally efficient, it runs as a post process, its performance benefits from the inclusion of high resolution information, and it can be refined much more easily.

Zaitchik, B.F., M. Rodell, and F. Olivera (2010). Evaluation of the Global Land Data Assimilation System using global river discharge data and a source to sink routing scheme, Water Resour. Res., 46, W06507, doi:10.1029/2009WR007811. published 10 June, 2010.

Figure 1: Gridded runoff (cm/yr) from the Global Land Data Assimilation System. Such results are useful for assessing spatial patterns of runoff generation, but they are not appropriate for direct comparison with gauge observations.

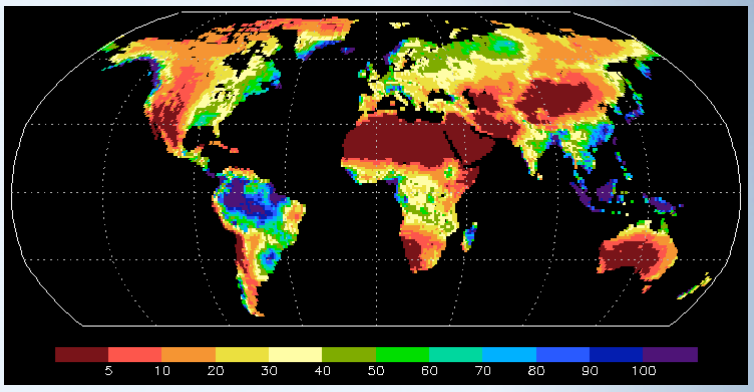

Figure 2: Schematic of the runoff routing scheme.

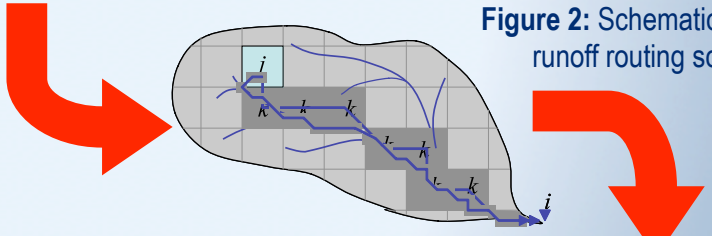

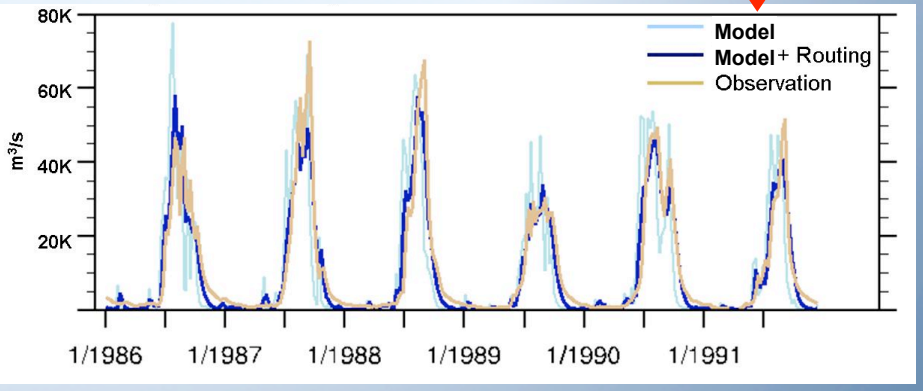

Figure 3: Time series of discharge (1,000 m^3/s) from the Ganges River. The modeled river discharge matches observations more closely after applying the routing scheme.

NEWS Publication Highlight

Papa, F., C. Prigent, F. Aires, C. Jimenez, W. B. Rossow, and E. Matthews (2010), Interannual variability of **surface water extent at the global scale**, 1993–2004, J. Geophys. Res., 115, D12111, doi: 10.1029/2009JD012674. **Published 19 June**.

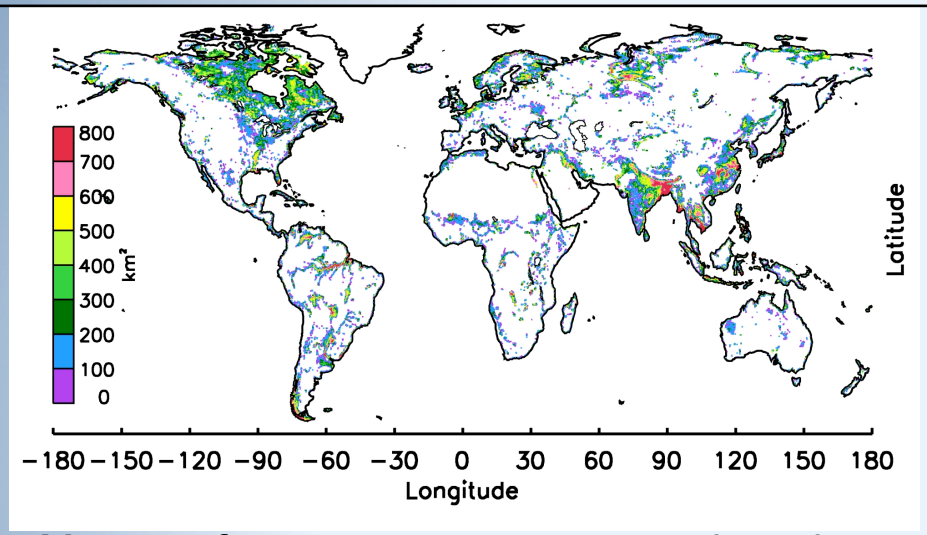

Mean surface water extent at annual maximum

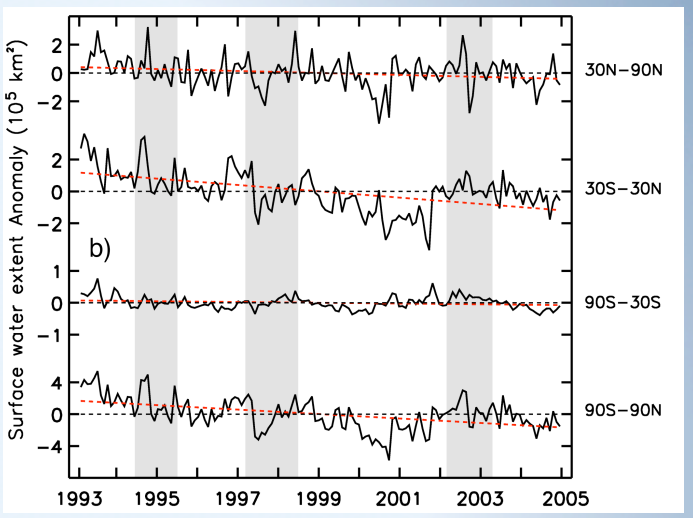

Interannual variations and trends 1993-2004 by latitude bands

Land surface waters play a primary role in the **global water cycle and climate**. As a consequence, there is a widespread demand for **accurate and long-term quantitative observations of their distribution over the whole globe**. This study presents the **first global data set** that quantifies the monthly **distribution of surface water extent** at ~25 km sampling intervals over **12 years (1993–2004)**. These estimates are generated from **complementary multiple-satellite observations**, including passive (Special Sensor Microwave Imager) and active (ERS scatterometer) microwaves along with visible and near-infrared imagery (advanced very high-resolution radiometer; AVHRR., In addition **to a large seasonal and interannual variability**, the new results show a **slight overall decrease in global inundated area between 1993 and 2004**, representing an **~5.7% reduction of the mean annual maximum in 12 years**. The **decrease** is mainly observed in the **tropics during the 1990s**. This new 12 year data set of global surface water extent represents an unprecedented source of **information for future hydrological or methane modeling**.

NASA ENERGY AND WATER CYCLE STUDY NEWS

Understanding complicated vertical cloud structure observed by CALIPSO and CloudSat for energy cycle

This study explains the process of merging CALIPSO and CloudSat derived vertical cloud profiles. Using CALIPSO and CloudSat derived cloud profiles, the paper also shows that the cloud cover, vertical overlapping probability, and cloud physical thickness can be related by simple relationships. The relationship provides a useful tool to understand complicated cloud structure for energy cycle.

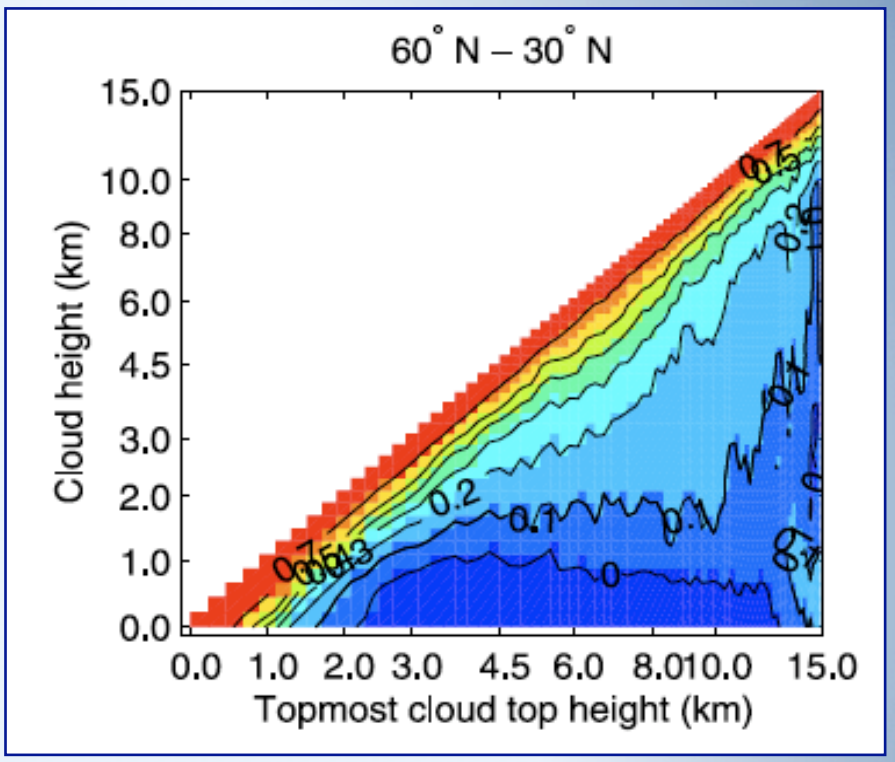

Probability of cloud occurrence as a function of the uppermost cloud top height. The monotonically decreases with the vertical distance from the cloud top, once a random probability of cloud overlap is taken into account. This allows us to establish a simplerelationship among cloud cover, vertical overlapping probability and cloud physical thickness.

Kato, S., S. Sun-Mack, W. F. Miller, F. G. Rose, Y. Chen, P. Minnis, and B. A. Wielicki (2010), Relationships among cloud occurrence frequency, overlap, and effective thickness derived from CALIPSO and CloudSat merged cloud vertical profiles, J. Geophys. Res., **115**, D00H28, doi:10.1029/2009JD012277

CALIPSO, CloudSat, CERES, and MODIS merged product (C3M) described in the paper is produced under the NASA Energy and Water cycle Study program. The product is available from http://eosweb.larc.nasa.gov/PRODOCS/ceres-news/table_ceres-news.html

A 10-yr climatology of cloud fraction and vertical distribution derived from both surface and GOES observations over the DOE ARM SGP site

Baike Xi, Xiquan Dong, Pat Minnis and Mandy Khaiyer, A 10-yr climatology of cloud fraction and vertical distribution derived from both surface and GOES observations over the DOE ARM SGP site, J. of Geophys. Res., 115, D12124, doi:10.1029/2009JD012800, 2010

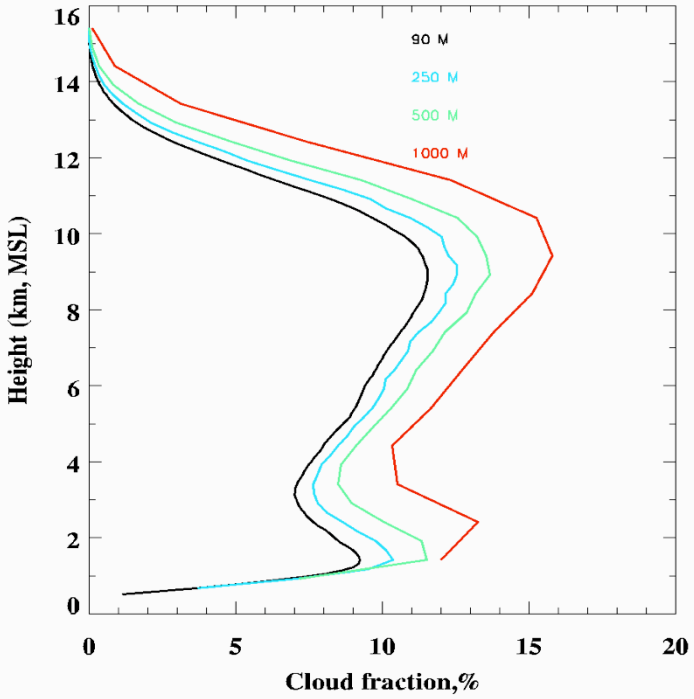

Left: Mean vertical distributions of CF derived from the ARM radar-lidar observations with a 5 min temporal resolution and vertical resolutions of 90, 250, 500, and 1000 m at the ARM SGP site, 1997–2006.

Right: Dependence on Clouds on Termporal and Spatial Resolution

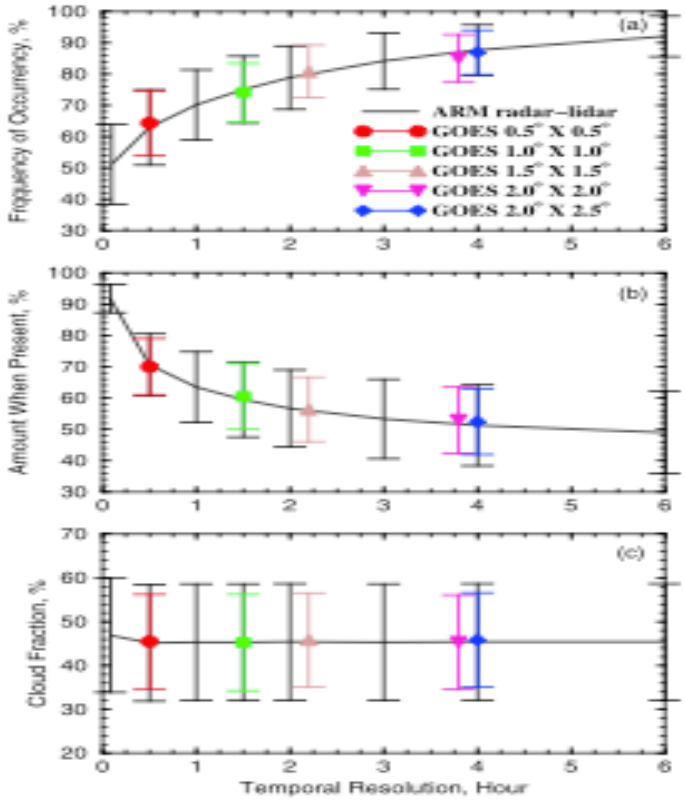

The assumed or computed vertical structures of cloud occurrence in GCMs is one of the main reasons why the different models predict a wide range of future climates. How accurately the surface-based narrow radar-lidar field-of-view (FOV) observations represent the large grid boxes used in GCMs remains an unresolved issue. **Researchers** from University of North Dakota and NASA Langley **used one decade of radar-lidar and Geostationary Operational Environmental Satellite (GOES) observations at the ARM Southern Great Plains (SGP) site to address this issue**, and provided what parameters are (not) comparable between surface and satellite observations**. These results should provide the most complete statistics, to date, of the long-term average cloud fraction and vertical distributions of clouds over the climatically important SGP site, and can be used as ground truth for both surface observers and satellite researchers to quantitatively understand and explain the differences between their observations and cloud truth. They should also be valuable for advancing our understanding of the vertical distributions of clouds and for enabling climate/forecast modelers to more fully evaluate their simulations and improve their parameterizations over the SGP.** 8/2/10